Computer Assisted Mechanics and Engineering Sciences, 8: 579–593, 2001.

Remarks on numerical estimation of the critical impact velocity in shear

Maciej Klósak[1,2], Tomasz Łodygowski[1] and Janusz R. Klepaczko[2]

[1] *Institute of Structural Engineering, Poznań University of Technology, ul. Piotrowo 5, 60-965 Poznań, Poland*

[2] *Metz University, Lab. of Physics and Mechanics of Materials, Ile du Saulcy, 57-045 Metz, France*

(Received March 3, 2000)

A phenomenon called the Critical Impact Velocity (CIV), which is directly related to material behavior under dynamic loads, is of special interest in this paper. Deformation trapping due to thermoplastic instability caused by the propagation of plastic waves is the main physical reasons for the CIV. This critical value of shear velocity should be considered as a material constant, but it is difficult to estimate due to complicated material response. Analytical approaches may only provide some preliminary estimates, because they are based on simple constitutive relations. On the other hand, experimental techniques are more reliable, but then there exist problems in specimen design. Numerical techniques such as FE method offer a possibility to treat the problem in a more general aspect.

Numerical results obtained in the environment of ABAQUS code demonstrate the role to be played by computer simulations as compared to the analytical and experimental findings. The CIV in shear is studied for the case of martensitic steel VAR4340, and the FE models are based on geometry of the Modified Double Shear specimen (MDS). Thus, the principal questions are formulated as follows: to which extent the analytical approach approximate the CIV, what is the role of experimental results and what information can be obtained after numerical simulations.

1. Preliminary remarks

The CIV in tension was already reported after experiments of Clark and Datwyler in 1938 [2] where a decrease of failure energy in tension tests at high impact velocities indicated on some unconventional behavior. A simple analytical approach to the phenomenon was presented by Karman and Duvez [5]. Concerning CIV in shear, the problem is more recent, and was signaled for the first time by Klepaczko [8]. The CIV in shear is caused by localization of plastic deformation in the form of Adiabatic Shear Bands (ABS). At high strain rates the conditions of deformation are nearly adiabatic which means that the mechanical work of plastic deformation is converted very rapidly into heat. When the process of deformation is localized the local heating of the material may be quite substantial and, as a consequence, due to thermal softening, the local plastic flow becomes unstable. Finally, this process of thermal coupling leads to the formation of ASB, a very narrow layer of shear deformation. Direction of the ASB is normally aligned with a local direction of maximum shear stress.

The phenomenon of CIV in shear has been first predicted by Litoński [14] and later independently included into the fragmentation modeling by Erlich, Curran and Seaman [4]. Simple analytical solution for CIV in shear have been discussed by Klepaczko [8]. Those studies confirm the experimental results that for some steels the CIV is around 100 m/s.

A numerical study of one-dimensional plastic shear wave propagation and its trapping in half-space of a nonlinear plastic material was considered by Wu and Freund [18]. The surface of the half-space was subjected to a time-dependent, but uniform on the surface, tangential velocity. The material was assumed with strain hardening, thermal softening and rate sensitivity of the flow stress.

It was found from the analysis by simple waves and by numerical calculations that a well-defined band of intense shear deformation appears adjacent to the surface. The representative profiles of particle velocity and strain were found near the surface for different strain rate sensitivities (linear and logarithmic). It was concluded that the band of intense shear deformation could be developed without any imperfection.

Recent experiments on construction and low-alloy steels with relatively new experimental technique of direct impact on Modified Double Shear specimen (MDS) [7], have revealed existence of the CIV in shear. At impact velocities of the order of 100 m/s plastic deformation in the form of ASB was always localized near the impact side of the sheared layer. The superposition of adiabatic shear banding and adiabatic plastic waves in shear is the main cause of such extremely fast localization.

Numerical studies of adiabatic shear banding by a quasi-static approach are quite numerous and they will not be discussed here, however, only few numerical studies are focused on adiabatic instability and localization at wide range of the nominal strain rates, for example [7, 8, 9]. Only the analysis which takes into consideration inertia effects, that is in plastic waves, may allow for CIV analyses. The numerical results presented in this paper have been inspired by experimental results obtained by Klepaczko [7]. Those results have permitted to obtain an experimental value of CIV. On the other hand, computer simulations have allowed for a wider examination of the problem, providing some interesting observations and proving high utility of those methods.

2. Simple analytical modeling of the CIV in shear

In order to analyze the CIV in shear the condition for stability $(\mathrm{d}\tau/\mathrm{d}\Gamma) = 0$ can be used, following [8]. This condition can be only satisfied in shear when the thermal heating leads to the thermal softening. If only one isothermal stress–strain curve $\tau = f(\Gamma)$ is assumed where τ is shear stress and Γ is shear gradient, in the adiabatic conditions due to the thermal softening, the tangent modulus becomes zero, $(\mathrm{d}\tau/\mathrm{d}\Gamma)_A = 0$, and in the limit the plastic strain propagates at zero speed. This notion permits for an analysis of CIV in shear by simple plastic waves.

As the first step the conditions of adiabatic instability in shear will be discussed. Assuming existence of the only one isothermal and one adiabatic shear stress–shear strain relation in the form $\tau = f(\Gamma)$ and the condition for stability during adiabatic shearing $\tau_A = f_A(\Gamma)$ leads to the formula

$$\left(\frac{\mathrm{d}\tau}{\mathrm{d}\Gamma}\right)_A = 0, \qquad (\dot{\Gamma}) = \text{const.} \tag{1}$$

A number of authors have used the stability criterion (1), for example [16], in order to find the instability strain Γ_c when the condition (1) is satisfied. The review of different formulae for $Gamma_c$ for different forms of constitutive relations was published by Dormeval [3].

Because many authors use constitutive relations in the form of multiplicative decomposition

$$\tau = f_1(T)\, f_2(\Gamma)\, f_3(\dot{\Gamma}), \tag{2}$$

where T is the absolute temperature, the strain-rate and temperature history effects are neglected, the stability criterion for adiabatic condition of deformation was derived using Eqs. (1) and (2) by Klepaczko [8].

It can be shown that condition (1) can be satisfied only for very specific processes of plastic deformations. One of them is adiabatic deformation at constant strain rate. Since only $f_2(\Gamma_c)$ is a function of the instability strain Γ_c. The explicit relation for $f_2(\Gamma_c)$ was derived by Klepaczko [8] in the following form,

$$f_2(\Gamma_c) = \left[-\frac{\left(\frac{\partial f_2}{\partial \Gamma}\right)}{\left(\frac{\partial f_1}{\partial T}\right)} \frac{\rho C_v}{f_3(\dot{\Gamma})(1-\xi)} \right]^{1/2}, \tag{3}$$

where $\xi(T,\Gamma)$ is a coefficient taking into account the stored energy in the material, $\rho(T)$ is the mass density and $C_v(T)$ is the specific heat at constant volume. In general, both ρ and C_v are functions of the absolute temperature T.

The expression $[\cdot]^{1/2}$ has real and imaginary parts. Inversion of $f_2(\Gamma_c)$ enables one to find Γ_c,

$$\Gamma_c = f_2^{-1}[\cdot]^{1/2}. \tag{4}$$

Existence of the real $f_2(\Gamma_c)$ is only possible if the expression $[\cdot]^{1/2}$ inside the square brackets is positive. Since ρ, C_v and $(1-\xi)$ must be always positive and the function of strain rate sensitivity, $f_3(\dot{\Gamma})$, is assumed also positive, the only term which may be negative is $(\partial f_2/\partial\Gamma)/(\partial f_1/\partial T)$. The most common case is the thermal softening which leads to negative value of $(\partial f_1/\partial T)$, of course, if $(\partial f_2/\partial\Gamma)$ is at the same time positive. The role of a positive rate sensitivity is quite interesting, that is if $f_3(\dot{\Gamma})$ is an increasing function of strain rate $\dot{\Gamma}$, the positive rate sensitivity has a negative effect on the onset of adiabatic instability, that is Γ_c is reduced when strain rate is increased.

By analogy to CIV in tension discussed by Klepaczko [6], it is possible to construct a model of the plastic wave trapping in shear [8], based on the criterion of adiabatic instability, Eqs. (1) and (3). According to the rate-independent theory of elastic–plastic wave propagation, as applied to shear deformation, the CIV in shear, denoted by v_c, is

$$v_c = \int_0^{\Gamma_c} C_{2p}(\Gamma)_{\dot{\Gamma}}\, \mathrm{d}\Gamma, \tag{5}$$

where shear occurs along x-axis and wave propagates along y-axis (perpendicular), Fig. 1. The wave speed is defined as

$$C_{2p}(\Gamma) = \left(\frac{1}{\rho}\frac{\mathrm{d}\tau}{\mathrm{d}\Gamma}\right)^{1/2}. \tag{6}$$

Equation (6) reduces to $C_2 = \sqrt{\mu/\rho}$ in the elastic case; where μ is the shear modulus and ρ is the density. In Eq. (5), Γ_c is defined by Eq. (4).

Finally, the Critical Impact Velocity in shear was given by Klepaczko in the following form,

$$v_c = \int_0^{\Gamma_c} \left\{\frac{f_1 f_2 f_3}{\rho}\left[\frac{1}{f_2}\left(\frac{\partial f_2}{\partial\Gamma}\right) + f_2 f_3\left(\frac{\partial f_1}{\partial T}\right)\frac{1-\xi}{\rho C_v}\right]\right\}^{1/2} \mathrm{d}\Gamma, \tag{7}$$

where the upper limit of integration is given by (4).

In order to estimate theoretical value of CIV for VAR4340 steel at room temperature, the analysis by simple waves was performed as it is summarized above. However, the structure of the constitutive relation has been changed, see Eq. (11) for VAR4340 steel presented further in this paper, with the material constants shown in Table 1. Since this approach is limited to only one $\tau(\Gamma)$ curve the strain rate assumed was $\dot{\Gamma} = 10^4 s^{-1}$. Integration of Eq. (7) can be divided into two steps,

$$v_c = C_2\Gamma_e + \int_{\Gamma_e}^{\Gamma_m} C_{2p}(\Gamma)\,\mathrm{d}\Gamma \qquad \text{with} \qquad C_2 = \left(\frac{\mu}{\rho}\right)^{1/2}. \tag{8}$$

For high-quality steels including VAR4340, the first term in Eq. (8) constitutes an important contribution to v_c (CIV in shear). For such steels the rate of strain hardening $(\partial\tau/\partial\Gamma)_A$ is substantially reduced and the second term is not so important. The two terms in Eq. (8) contribute to CIV as follows: $v_{ce} = 51.1$ m/s and $v_{cp} = 57.0$ m/s, thus $v_c = 108.1$ m/s.

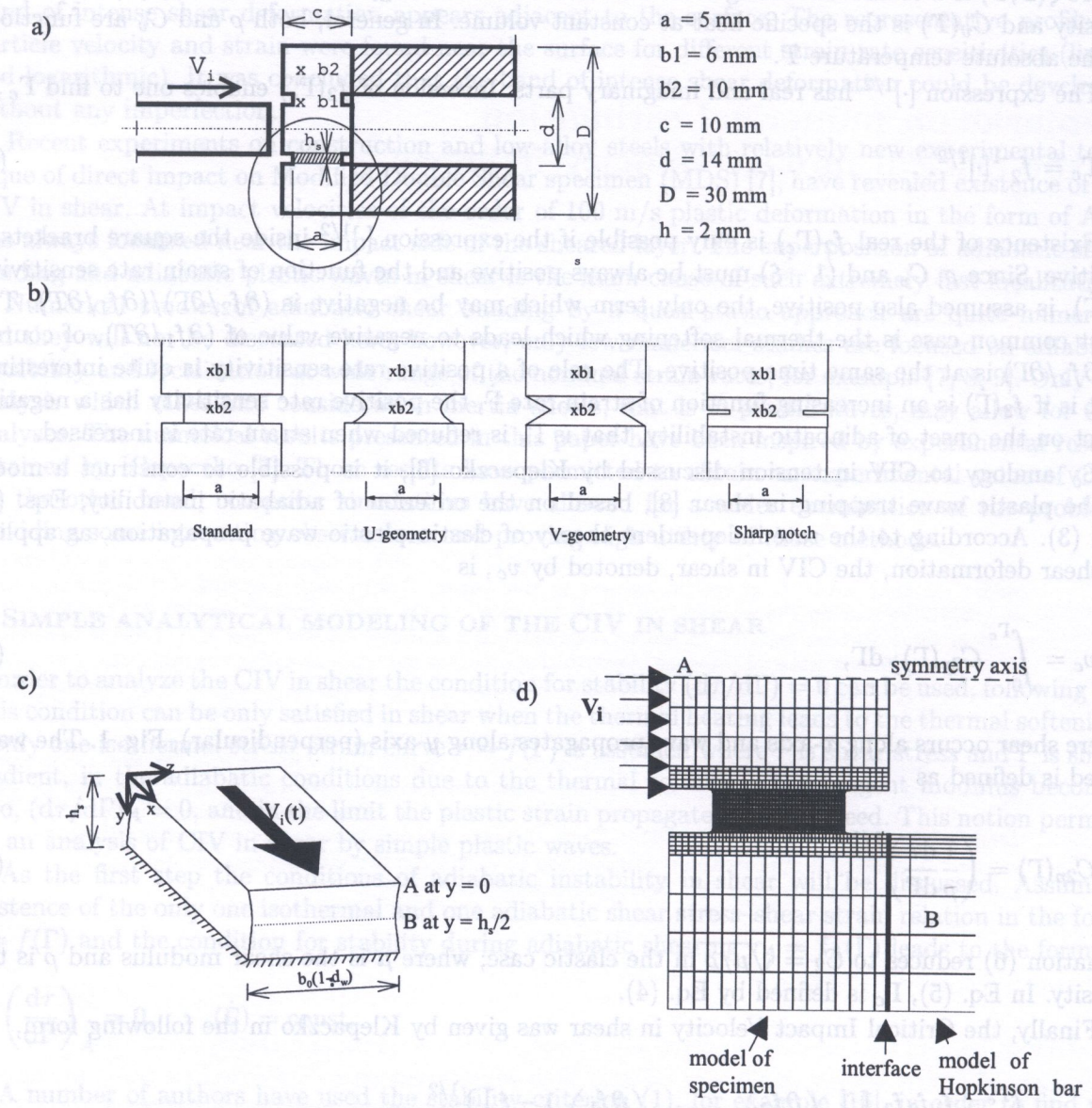

Fig. 1. Experimental technique od duble shearing; a) scheme of experimental configuration, b) shapes of specimens, c) FE modeling – Model I, d) FE modeling – Model II

Table 1. Material constants for VAR4340 steel, ~ 50 HRC

Const.	Value	Unit	Const.	Value	Unit
B	1493.0	MPa	A	$5.047 \cdot 10^{-4}$	1/K
μ	80770.0	MPa	C	$1.036 \cdot 10^{-7}$	$1/K^2$
ν	0.39	–	D	2914.0	K
n	Eq. (13)	–	τ_0	622.0	MPa
n_0	0.1354	–	β	0.9	–
m	2.78	–	λ	38.0	W/mK
T_0	300.0	K	ρ	7890.0	kg/m^3
Γ_0	$1.6 \cdot 10^{-3}$	–	C_v	460.0	J/kgK
$\dot{\Gamma}_0$	10^6	1/s	T_m	1812.0	K

3. EXPERIMENTAL TECHNIQUE OF DOUBLE SHEAR – A TOOL FOR CIV ESTIMATION

Experimental results should be treated as a base for a problem to be solved. Therefore, the experimental technique must provide reliable data. The first experimental results of Klepaczko [7] concerning CIV on low-alloy steels have encouraged to extend this method to other steels, including VAR4340. A general idea of the experimental technique based on the direct impact on MDS specimen is shown in Fig. 1a. The MDS specimen is loaded by the round projectile $\Phi = 10$ mm with the impact velocity V_i, $1 \leq V_i \leq 200$ m/s. The MDS specimen is supported by the Hopkinson tube where the transmitted wave is measured. Displacement of the central part of the MDS specimen is measured as a function of time by an optical displacement transducer. There are two shearing zones in the specimen, the height of each is $h_s = 2.0$ mm, the length $a = 5.0$ mm and the thickness $b = 6.0$ mm. The initial conditions are such that the imposed velocity on the shearing layers occurs at the surfaces closer to the projectile. Since displacement of the Hopkinson tube is relatively small, the external shear layers practically do not move, and the Hopkinson tube can be assumed as a rigid support.

In order to study stress concentrators the external dimensions of the MDS specimen are unchanged, only the shearing zone is modified. Four different shapes of that zone have been used, Fig. 1b. The purpose to vary the geometry of the shear zones in such a way is to analyse the effect of stress concentrators on the material resistance to critical conditions in shear. Only first two geometries (standard and U-geometry) seem to be useful for the CIV estimation. Some recent results for 4340 steel $\sim$ 50 HRC are presented below, following Klepaczko [8]. The value estimated for the CIV for this steel is $\sim$ 130 m/s. Typical curves shear stress versus shear strain obtained from experiments are presented in Fig. 2. These results indicate for a substantial change in specimen behaviour when the impact velocity is increased. When stresses become higher the nominal strain at failure decreases. In order to estimate the CIV for such cases, the results must be analysed further. In Fig. 3 is shown the plastic energy dissipated up to failure as a function of the nominal strain rate which is proportional to the impact velocity. These curves were obtained after integration of the τ–Γ curves. The failure energy starts to diminish at certain level of nominal strain rate which may indicate that the CIV was reached. Similar observation was reported by Clark and Datwyler [2] in tension tests. It seems that the CIV might correspond to the value of impact velocity at which the energy starts to diminish. This fact can be well identified for standard and U-type geometries. But sharp stress concentrators for the V-type geometry enforce more brittle failure and obscures CIV estimation. It is concluded that only standard and U-geometries have adequate shapes to study the CIV estimation. The complete interpretation of such results are given in the following parts of this paper.

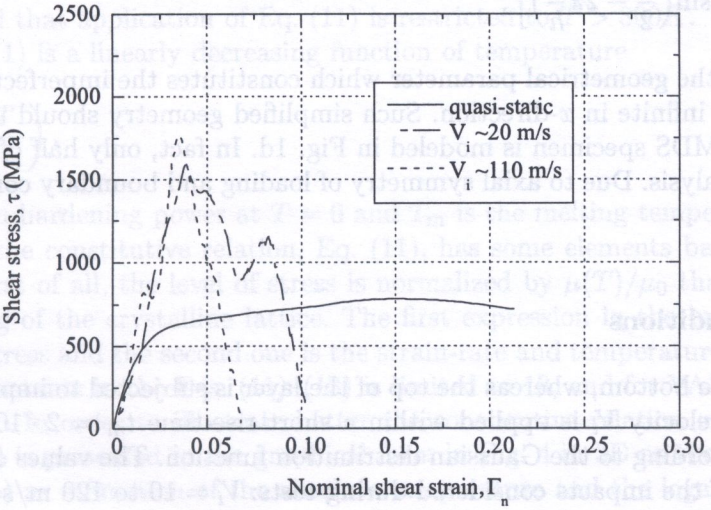

Fig. 2. Set of stress–strain curves for different impact velocity – standard geometry

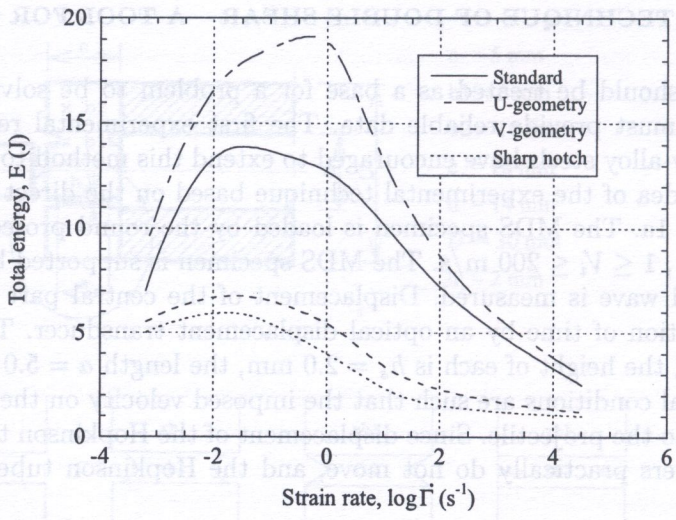

Fig. 3. Mean values of total inelastic energy dissipated up to failure for different shapes of stress concentrators

4. Computer simulation of double-shear impact test

4.1. Finite element modeling

Recent experimental results have served as a starting point for further computer simulations. The simulations have been performed using the environment of ABAQUS/Explicit code [1]. The geometry of the MDS specimen has imposed the FE model. The problem has been considered at two stages: Model I is a simplification of the MDS specimen, i.e. only the shearing zone was modeled. On the other hand, Model II is a complete MDS geometry representation which retains real dimensions with more complex boundary conditions. Both approaches have their advantages. The simplified geometry of Model I permits to observe more easily instability processes and the CIV phenomenon. Model II is closer to experimental reality and gives idea about efficiency of the experimental technique when dealing with the CIV as well as provides information about usefulness of the FE method itself. Both Models I and II are presented in Fig. 1. In Fig. 1c is shown the infinite layer. The height of the layer is the same as of the shearing zone in the MDS specimen, $h_s = 2.0$ mm, the profile changes along the y-direction according to the imperfection function

$$b(y) = b_0 \left[1 + \delta_w \sin\left(\frac{\pi}{2} - 2\pi\frac{y}{h}\right)\right], \tag{9}$$

where $\delta_w = 0.005$ is the geometrical parameter which constitutes the imperfection of 1%. Moreover, the layer is assumed infinite in x-direction. Such simplified geometry should useful to estimate the CIV. The complete MDS specimen is modeled in Fig. 1d. In fact, only half of the specimen is considered in the FE analysis. Due to axial symmetry of loading and boundary conditions, symmetrical impact is assumed.

4.2. Boundary conditions

Model I is fixed at the bottom, whereas the top of the layer is subjected to impact. In both Models I and II, the impact velocity V_i is applied within a short rise-time $t_m = 2 \cdot 10^{-6}$ to $2 \cdot 10^{-7}$ s, the shape is assumed according to the Gaussian distribution function. The values of the impact velocity V_i cover the range of the impacts considered during tests: $V_i = 10$ to 120 m/s or higher.

Model II takes into account the interface: specimen – Hopkinson tube. This support is modeled using two contact surfaces which allow for free movement (separation) of the specimen and the

Hopkinson tube. Both Models I and II are 2-dimensional. Model I is assumed as "plane strain". Model II is assumed as "plane stress"; 4-node elements with reduced integration are used.

4.3. Material

It is well known that an adequate constitutive relation is the essential condition for reliable FE results. A constitutive relation applied to the problems of plastic instability coupled with temperature must reflect properly the effect of strain hardening, temperature sensitivity and rate sensitivity at high strain rates on the flow stress. The constitutive relation applied to the problem considered has specially been developed to model experimental results for VAR 4340 steel [17], as well as other data were used for similar steels. After careful analyses of available experimental data for VAR 4340 steel of hardness $\sim$ 50 HRC the following general form is chosen,

$$\tau = f_1(T)\,[f_2(T)\,f_3(\Gamma, T) + f_4(\dot{\Gamma}, T)], \tag{10}$$

where f_i are the functions of plastic shear strain Γ, shear strain rate $\dot{\Gamma}$ and absolute temperature T. Relation (10) is treated as a first approximation to the constitutive modeling. The explicit form is assumed as follows,

$$\tau = \frac{\mu(T)}{\mu_0}\left[B\left(\frac{T}{T_0}\right)^{-\nu}(\Gamma_0 + \Gamma_p)^n + \tau_0\left(1 - \frac{T}{D}\log\frac{\dot{\Gamma}_0}{\dot{\Gamma}}\right)^m\right], \qquad T < T_c \quad \text{and} \quad \dot{\Gamma} > \dot{\Gamma}_c. \tag{11}$$

If $T > T_c$ then $\tau_0(*) = 0$ with

$$\left(\frac{T}{D}\log\frac{\dot{\Gamma}_0}{\dot{\Gamma}}\right) = 1,$$

where B, μ_0, ν, n, m are, respectively, the modulus of plasticity, the shear modulus at $T = 300$ K, the temperature index, the strain hardening exponent and the logarithmic rate sensitivity; D, T_0, Γ_0 and $\dot{\Gamma}_0$ are normalization constants. The temperature dependence of the shear modulus is given by

$$\mu(T) = \mu_0(1 - AT^* - CT^{*2}), \qquad T^* = T - 300, \tag{12}$$

where A and C are material constants.

It should be noted that application of Eq. (11) is restricted to $T > 300K$. The strain hardening power $n(T)$ in Eq. (11) is a linearly decreasing function of temperature

$$n(T) = n_0\left(1 - \frac{T}{T_m}\right), \tag{13}$$

where n_0 is the strain hardening power at $T = 0$ and T_m is the melting temperature.

The structure of the constitutive relation, Eq. (11), has some elements based on the materials science approach. First of all, the level of stress is normalized by $\mu(T)/\mu_0$ that takes into account the thermal softening of the crystalline lattice. The first expression in the brackets of Eq. (11) is simply the internal stress and the second one is the strain-rate and temperature-dependent effective stress. Number of constants in the Eqs. (11)–(13) is limited to 18, and for VAR 4340 steel they are assembled in Table 1. In order to illustrate better the constitutive relation used in the numerical calculations, Eq. (11) is presented in the graphical form in Fig. 4 in 3D as the yield stress in shear (plastic strain is zero) as a function of the absolute temperature and the logarithm of shear strain rate. The effect of strain rate on the shear yield limit is more intense at lower temperatures, this is a typical behavior for steels. The solid line in Fig. 4 shows the limit of the $f_4(\dot{\Gamma}, T)$ term in Eq. (11).

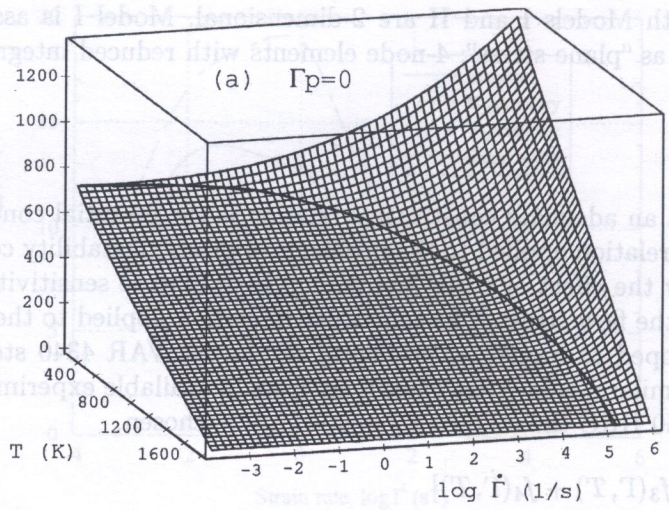

Fig. 4. Evolution of the shear stress as a function of temperature and strain rate

A more exact analysis of the constitutive relation is discussed elsewhere [13]. The well-possedness of the constitutive relation has been assured by introduction of strain rate sensitivity, for example [15].

Failure criteria based on the critical shear strain and the critical strain energy density had been implemented in the code. Both approaches yielded similar results. The important difference in material definition in both models is that in Model I no failure criterion is implemented. Material is then plastified with no limit. It enables to find CIV more easily and the result is not perturbed by the material damage.

4.4. Results of FE simulations

For Model I the evolution of deformations in the layer as a function of the impact velocity is shown in Fig. 5. A high strain rate ($\sim 10^4$ s^{-1}) still leads to deformation fields such as presented in Fig. 5a. This mode of deformation is typical for "quasi-static" behaviour. For higher impact velocities, the behavior of layer is completely changed, the plastic deformations are localised at the upper surface. This indicates that CIV has been reached. Another representation of the CIV phenomenon is given in Fig. 6. The spatial distribution of strain rates $\dot{\Gamma}_n$ at the end of localization assumed as $\partial\tau/\partial\Gamma_n = -7{\cdot}10^3$ MPa for four impact velocities clearly shows evolution in the behavior. Local trapping of plastic deformations near the impact surface has produced local strain rates of the order of 10^6 s^{-1}. It is interesting to note in Fig. 6 that local maximum of strain rate occurs for high impact velocities, but at velocities inferior of the CIV. This maximum is shifted off the center, so the geometrical imperfection assumed has no longer significant influence. This is due to propagation and superposition of plastic waves in the layer interior. Similar tendency is observed when the local temperatures are concerned. The increase of local temperature reaches high value, up to 700 K.

This has been confirmed by SEM observations for VAR4340 steel [7]. The most important observation is that the $\tau_A(\Gamma_n)$ reconstituted curves differ substantially at different impact velocities. This is demonstrated in Fig. 7. In the range of lower impact velocities, the $\tau_A(\Gamma_n)$ curves reflect a real behaviour of material; this is true up to $\sim$ 40 m/s. The curves determined at this velocity show a characteristic stress peak at very small strains. In addition, the initial slope in the "elastic" range becomes steeper than predicted by the shear modulus. This is due to interaction of plastic waves and the adiabatic instability near the upper surface of the layer. When the impact velocities are still higher, the maximum of shear stress occurs at very small nominal strains. Finally, Fig. 8 shows the total fracture energies estimated at different impact velocities. The energy has been es-

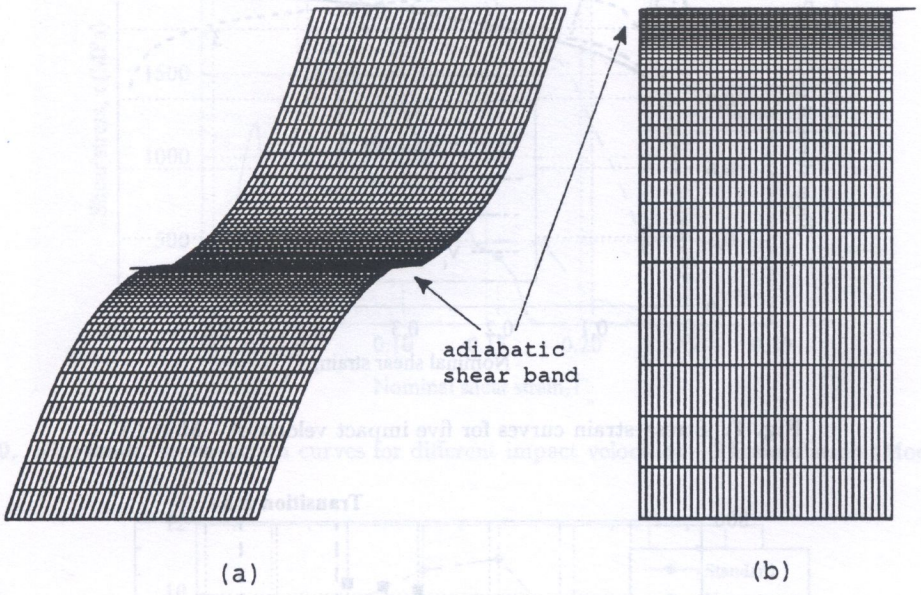

Fig. 5. Displacement fields for two impact velocities: a) $V_i = 40m/s$, b) $V_i = 130m/s$

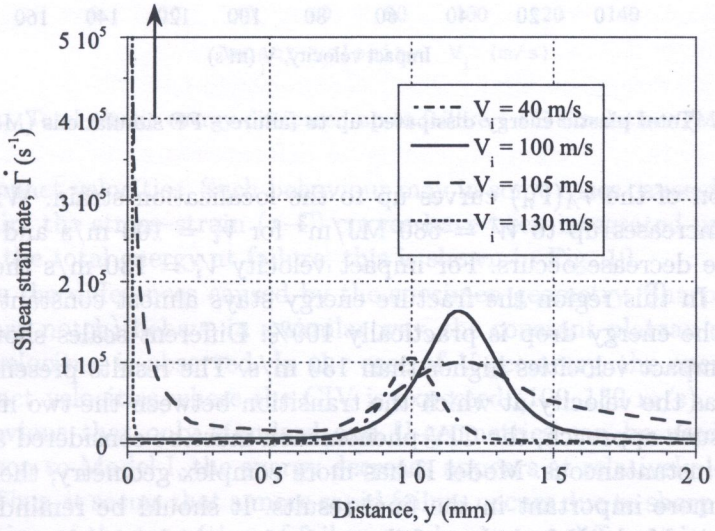

Fig. 6. Spatial distribution of strain rate at failure for different impact velocities (the impact occurs at the left side)

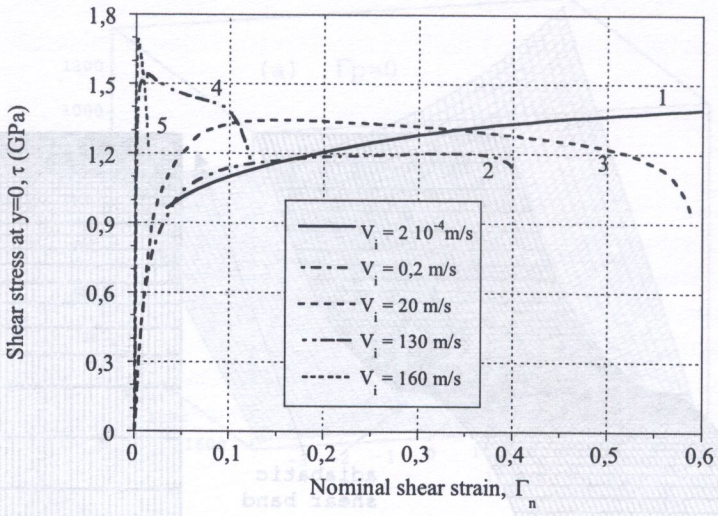

Fig. 7. Stress–strain curves for five impact velocities – Model I

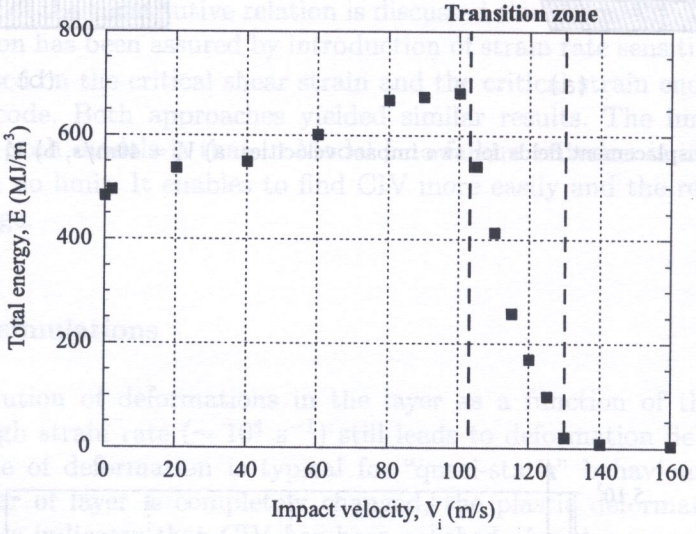

Fig. 8. Total plastic energy dissipated up to failure – FE simulations (Model I)

timated by integration of the $\tau_A(\Gamma_n)$ curves up to the localization strain. Within the first region the fracture energy increases up to $W = 680$ MJ/m^3 for $V_i = 100$ m/s and next, in the second region, a considerable decrease occurs. For impact velocity $V_i = 130$ m/s the energy reaches the level of ~ 8 MJ/m^3. In this region the fracture energy stays almost constant on the level from 6 to 8 MJ/m^3. Thus, the energy drop is practically 100%. Different scales should be used to show the energy level for impact velocities higher than 130 m/s. The results presented suggest that the CIV may be defined as the velocity at which the transition between the two modes of deformation appears; (Fig. 5). In such approach, the CIV phenomenon must be considered as a process in which this transition is not instantaneous. Model II has more complex geometry, therefore, the geometry effect appears to be more important in the final results. It should be reminded that constitutive relation implemented in Model II includes a failure criterion which models quasi-brittle behavior of VAR4340 steel, ~ 50 HRC. The global response of both models must be then different.

Figure 9 shows the nominal stress–strain (τ–Γ) curves, for only the standard geometry, at different impact velocities. An analogy with Fig. 7 (Model I) is evident: the failure appears earlier when impact velocities become sufficiently higher. It is important to mark on those curves the points corresponding to the instant of failure. It is concluded that the analysed specimen becomes more

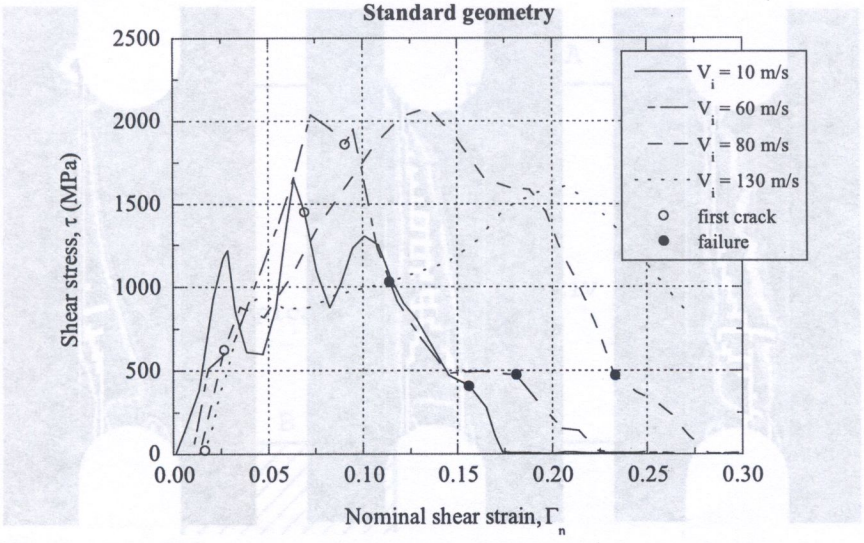

Fig. 9. FE results: stress–strain curves for different impact velocities – FE simulation (Model II)

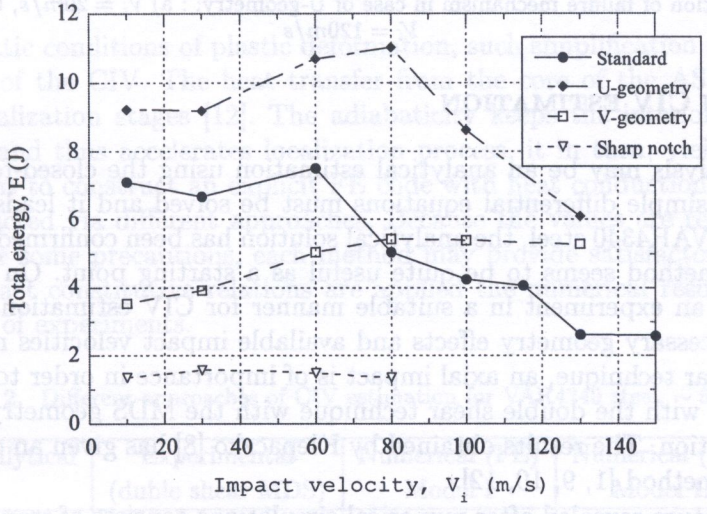

Fig. 10. Total plastic energy dissipated up to failure – FE simulations (Model II)

damaged at higher impact velocities. Such behaviour may in some cases cause difficulties in a proper CIV estimation. Again, the stress–strain (τ–Γ) curves have been integrated up to the failure point in order to calculate the total energy at failure, this is shown in Fig. 10.

This demonstrates the differences caused by the specimen geometry. Sharp stress concentrators (V-geometry and sharp notch) behave in a similar way, the constant plateau of energy throughout all range of impact velocities is observed. In the case of V-geometry, the energy even increases in certain range of impact velocities where the CIV is expected (100–130 m/s). This is typical effect of geometry. It is obvious that only standard and U-geometries can be used in CIV estimation. However, in comparison to Model I, the energy decrease appears at relatively low impact velocities, lower then the CIV. Thus, it seems that a more rapid failure occurs due to sharp stress concentrators. A perfect demonstration of the transition of failure mechanism at different impact velocities for U-geometry is shown in Fig. 11. For moderate impact velocities (10 m/s to 80 m/s), the initiation of the ASB occurs in the smallest cross section. On the other hand, for higher impact velocities, close to the CIV ($V_i \sim 130$ m/s), the ASB first appears in the cross section near the impact side. It is interesting to note a tendency in triggering of parallel shear bands that appears at specified impact velocity ($V_i \sim 80$ m/s), which indicates on an interplay between two modes of failure.

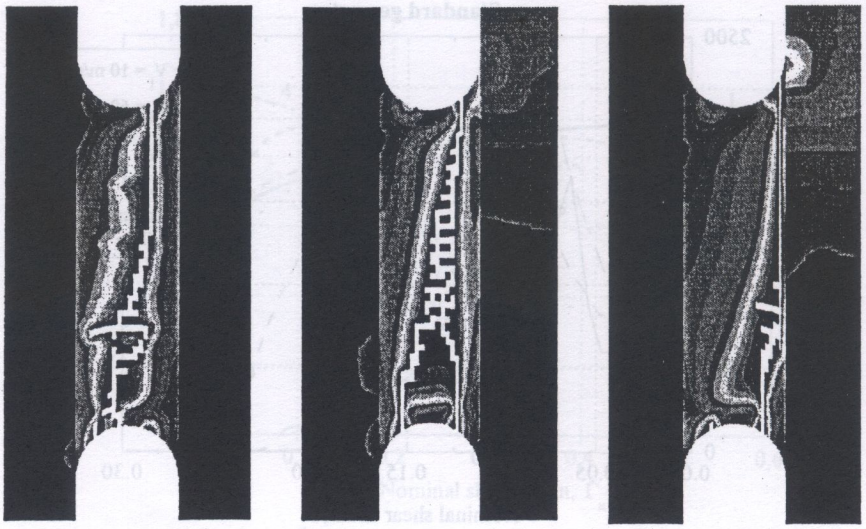

Fig. 11. Transition of failure mechanism in case of U-geometry: : a) $V_i = 20m/s$, b) $V_i = 80m/s$, c) $V_i = 120m/s$

5. Discussion on CIV estimation

The first step in analysis may be an analytical estimation using the closed-form solution. In such case, only relatively simple differential equations must be solved and it leads to a certain level of simplicity. In case of VAR4340 steel, the analytical solution has been confirmed by further numerical evaluations, so the method seems to be quite useful as a starting point. On the other hand, it is important to design an experiment in a suitable manner for CIV estimation. The specimen must be then free of unnecessary geometry effects and available impact velocities must exceed the CIV. In case of double shear technique, an axial impact is of importance in order to obtain reliable data. The results obtained with the double shear technique with the MDS geometry encourage for using it for the CIV estimation. The results obtained by Klepaczko [8] has given an occasion to model the problem by the FE method [1, 9, 10, 12].

The important feature revealed after numerical simulations consists of transition of the displacement and deformation fields. Both Model I and II have indicated a strong effect of the impact velocity above $V_i = 40$ m/s. A complete change of deformation mode above such specific impact velocity was found. This occurs near the CIV. It has been stated that CIV may be considered as a process (Model I), i.e. the CIV is defined within a small range of impact velocities rather than that given as one exact value. Of course, such statement is a consequence of the geometry effect, but this cannot be avoided in experiments and in numerical models of real specimens. The CIV is sensitive to material proprieties like strain hardening, temperature and strain rate sensitivity. For example, a material that reveals temperature sensitivity of strain hardening exponent may show quite different CIV values at different temperatures [6].

The schematic picture shown in Fig. 12 demonstrates the transition from "normal" to the CIV behavior. For the U-geometry the transition is similar, Fig. 11. Apparently, these results give satisfactory value of the transition which corresponds to the impact velocities close to 100 m/s and 120 m/s, respectively for standard and U-geometry. This seems quite a good estimation of the CIV. Different values for two other specimen geometries (V and I, Fig. 10) indicate on a strong geometry effect.

The user of FE programs must be conscious of consequences of anomalous modeling. Numerical discrepancies may be introduced by mesh alignment and mesh density, this can even completely change the results, for example [11]. Another important point in the numerical simulation is the

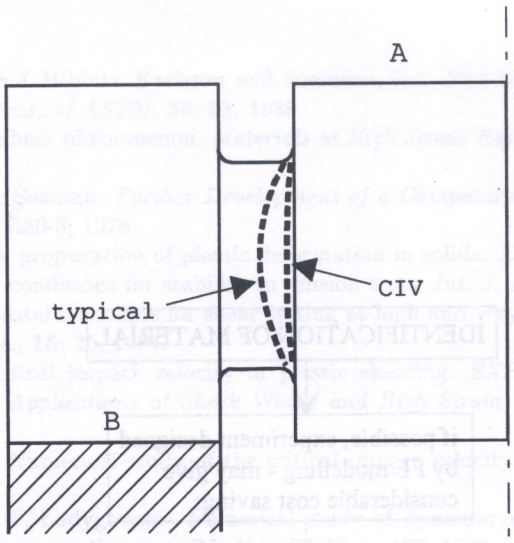

Fig. 12. Schematic shape of adiabatic shear bands produced in double shear experiment with MDS specimen

assumption of adiabatic conditions of plastic deformation, such simplification may slightly decrease the estimated value of the CIV. The heat transfer from the core of the ASB may be important during advanced localization stages [12]. The adiabaticity keeps the interior temperature higher than that in reality and thus accelerates localization process, it in turn, yields lower CIV values. It would be important to construct an explicit FE code with heat conduction. Table 2 summarises the CIV values predicted via different approaches. Because the values are relatively close, it may be stated that, under some precautions, each method may provide satisfactory results. It is clear, when correct and exact constitutive relations are applied the numerical results can be extremely useful in verification of experiments.

Table 2. Different approaches of CIV estimation for VAR4340 steel, ~ 50 HRC

Analytical	Experimental (duble shear MDS)	Numerical (FE) Model I	Numerical (FE) Model II
108.1 m/s	~130 m/s	103–130 m/s	100–120 m/s

The main conclusion is presented in the form of the following flow-chart (next page), where it is intended to place all necessary steps in the CIV estimation, or in general, how to deal with plastic instabilities in dynamics. The role of experiment should be predominant, however, new possibilities are offered by numerical techniques (software and hardware). The following picture presents how the both experiments and numerical simulations interact in the process of searching the properties and identification of material parameters. The future lies in the so called hybrid approach, that is experiment confronted with numerical methods via precise constitutive relations.

ACKNOWLEDGMENT

This paper is partly based on the PhD thesis of the first co-author. He expresses his thanks to the two other co-authors for their guidance. The Thesis has been prepared in the framework of the French-Polish co-operation, supported by the French Ministry of Foreign Affairs and the Poznan University of Technology. The computations were partially performed in Poznan Supercomputing and Networking Center.

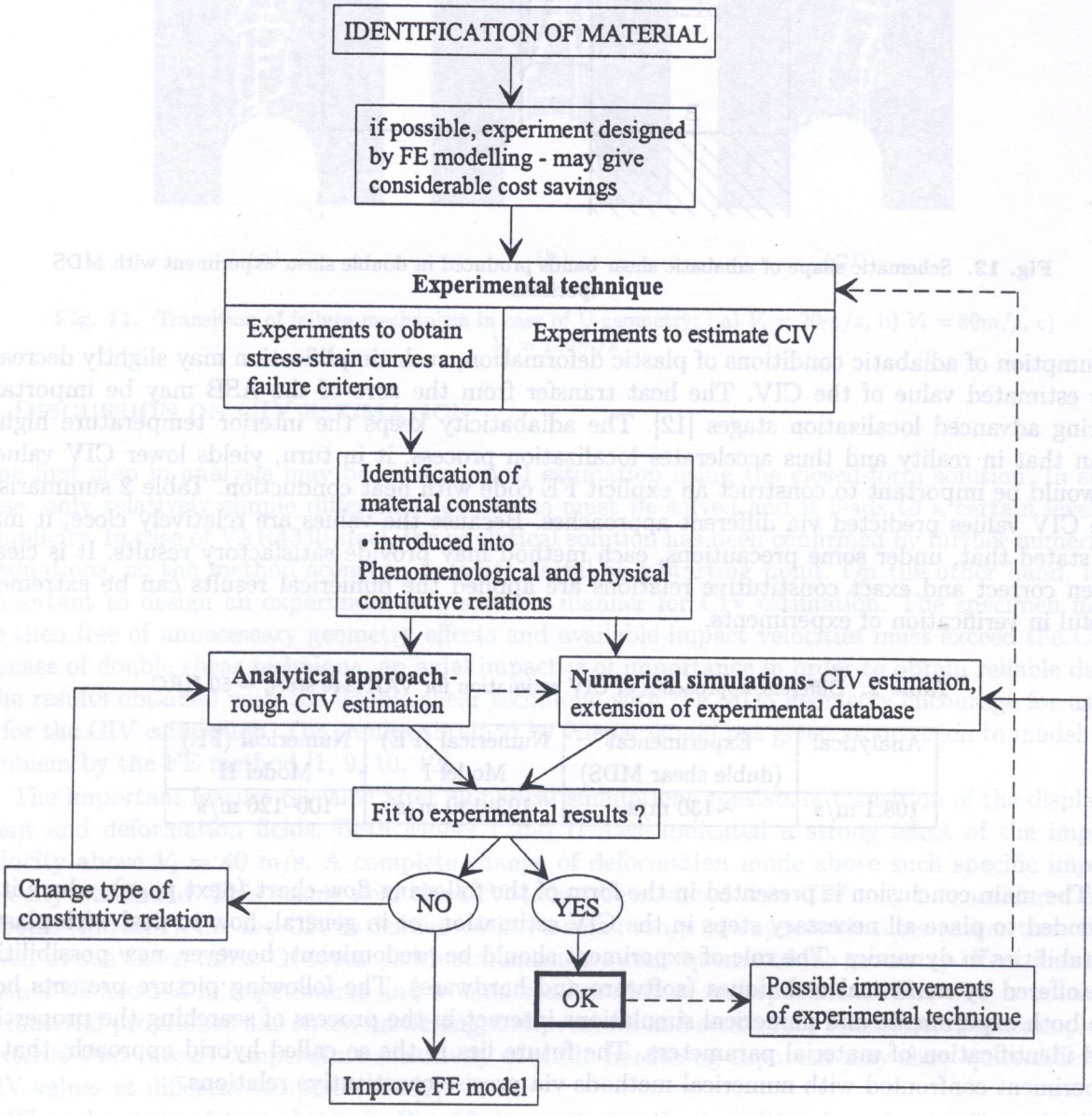
IDENTIFICATION OF MATERIAL
if possible, experiment designed by FE modelling - may give considerable cost savings
Experimental technique
Experiments to obtain stress-strain curves and failure criterion
Experiments to estimate CIV
Identification of material constants
• introduced into Phenomenological and physical contitutive relations
Analytical approach - rough CIV estimation
Numerical simulations- CIV estimation, extension of experimental database
Fit to experimental results ?
Change type of constitutive relation
NO
YES
OK
Possible improvements of experimental technique
Improve FE model

REFERENCES

[1] *ABAQUS Manual, Version 5.8.* Hibbitt, Karlsson and Sorensen, Inc., Providence, USA, 1998.

[2] D.C. Clark, G. Datwyler. *Trans. of ASTM*, **38**: 98, 1938.

[3] R. Dormevel. The adiabatic shear phenomenon. *Materials at High Strain Rates*, 47. Elsevier Appl. Sci., London, 1987.

[4] D.C. Erlich, D.R. Curran, L. Seaman. *Further Development of a Computational Shear Band Model.* SRI International Report, AMMRC TR80-3, 1978.

[5] T. Karman, P.E. Duvez. The propagation of plastic deformation in solids. *J. Appl. Phys.*, **21**: 987, 1950.

[6] J.R. Klepaczko. Generalized conditions for stability in tension tests. *Int. J. Mech. Sci.*, **10**: 297, 1968.

[7] J.R. Klepaczko. An experimental technique for shear testing at high and very high strain rates, the case of mild steel. *Int. Journ. Impact Eng.*, **15**: 25, 1994.

[8] J.R. Klepaczko. On the critical impact velocity in plastic shearing. *EXPLOMET'95, Proc. Int. Conf. On Metallurgical and Materials Applications of Shock Waves and High Strain Rate Phenomena*, p. 413. Elsevier Science, Amsterdam, 1995.

[9] J.R. Klepaczko, M. Klósak. Numerical study of the critical impact velocity in shear. *Eur. J. Mech. A/Solids*, **18**: 93, 1999.

[10] J.R. Klepaczko, M. Klósak, T. Łodygowski. Numerical study of dynamic instabilities in high-speed shearing. *Proc. ABAQUS Users' Conference, Newport, RI, May 27–29*, p. 407, 1998.

[11] M. Klósak. *Simulations Numériques de la Localisation Plastique dans les Aciers Martensitiques Chargés par Impact.* PhD Thesis, LPMM – Metz University, 1999.

[12] M. Klósak. Numerical simulation of the dynamic shear experiment accounting for heat conduction effects. *XIV Polish Conference on Computer Methods in Mechanics, Rzeszów, May 26–28*, p. 155, 1999.

[13] M. Klósak, J.R. Klepaczko. Numerical study of the critical impact velocity in shear. *Final Technical Report for the US Army European Res. Office*, DAJA N68171-95-C-9071, Appendix No 1. LPMM, Metz University, France, 1996.

[14] J. Litoński. Private communication, 1982.

[15] T. Łodygowski. On avoiding of spurious mesh sensitivity in numerical analysis of plastic strain localization. *Computer Assisted Mechanics and Engineering Sciences*, **2**: 231–248, 1995.

[16] R.F. Recht. Catastrophic thermoplastic shear. *J. Appl. Mech.*, **86**: 189, 1964.

[17] S. Tanimura, J. Duffy. *Strain Rate Effects and Temperature History Effects for Three Different Tempers of 4340 VAR Steel.* Brown University, Army Research Office, USA, Report No. DAAG 29-81-K-0121/4, 1984.

[18] F.H. Wu, L.B. Freund. Deformation trapping due to thermoplastic instability in one-dimensional wave propagation. *J. Mech. Phys. Solids*, **32**: 119, 1984.